ACS OMEGA

http://pubs.acs.org/journal/acsodf

Article

Discovery and Optimization of Highly Potent and Selective AT_2R Antagonists to Relieve Peripheral Neuropathic Pain

Yanghui Guo,* Xiangui Huang, Weiwei Liao, Lichen Meng, Daiwang Xu, Cheng Ye, Lei Chen, and Taishan Hu*

Cite This: *ACS Omega* 2021, 6, 15412−15420

Read Online

ACCESS | Metrics & More | Article Recommendations | Supporting Information

ABSTRACT: The angiotensin II type 2 receptor (AT_2R) has attracted much attention as a potential target for the relief of neuropathic pain, which represents an area of unmet clinical need. A series of 1,2,3,4-tetrahydroisoquinolines with a benzoxazole side-chain were discovered as potent AT_2R antagonists. Rational optimization resulted in compound **15**, which demonstrated both excellent antagonistic activity against AT_2R *in vitro* and analgesic efficacy in a rat chronic constriction injury model. Its favorable physicochemical properties and oral bioavailability make it a promising therapeutic candidate for neuropathic pain.

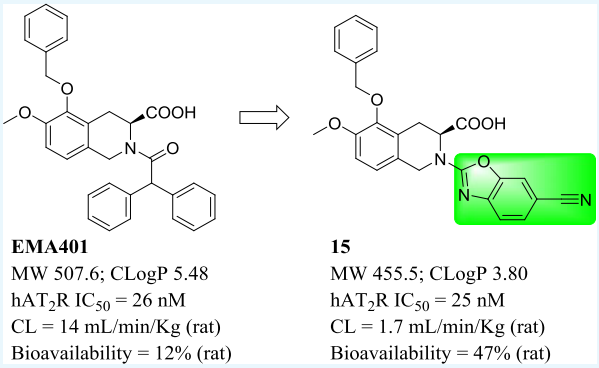

INTRODUCTION

Endogenous angiotensin II plays an important role in the renin-angiotensin system via two types of receptors, AT_1R and AT_2R, which only share approximately 34% sequence identity.[1,2] The two receptors have similar binding affinities to angiotensin II but differ in their functions. AT_1R serves as a key regulator of blood pressure and is a validated drug target with several antagonists approved as the well-known category of antihypertensives (valsartan, irbesartan etc.), while the function of AT_2R has remained enigmatic. Diverse biological functions of AT_2R have been reported and are often biological in context and cell- and tissue-dependent.[3,4] One of the profound effects is that activation of AT_2R by agonists, such as **C21**, demonstrated antifibrotic effects and promoted tissue protection in cardiovascular and renal diseases.[5−7] On the other hand, a growing number of studies suggest that AT_2R is involved in pain modulation,[8] and AT_2R antagonists could relieve peripheral neuropathic pain in animal models. Therefore, the AT_2R has drawn considerable attention as a new therapeutic target for treatments of different diseases. Neuropathic pain is caused by a lesion or disease affecting the somatosensory nervous system, either centrally or in the periphery.[9] The population prevalence of neuropathic pain is estimated to lie between 6.9 and 10%.[10] Neuropathic pain is common in cancer pain, diabetic neuropathy, postherpetic neuralgia, and trigeminal neuralgia, among others.[11] The pathophysiology of neuropathic pain is not well defined. The deficient mechanistic understanding of neuropathic pain, which is poorly managed by currently available drugs due to limited efficacy and tolerability, has undoubtedly impeded the discovery of effective analgesics.[12−15]

Recently, an oral small-molecule AT_2R antagonist, **EMA401** (Figure 1), has been reported to show analgesic efficacy in animal models and in a phase II clinical trial for neuropathic pain.[16−21] **EMA401** is a potent AT_2R antagonist with high selectivity over AT_1R. However, it had only moderate drug exposure and oral bioavailability in rats.[17] In addition, clinical pharmacokinetic (PK) data indicated that large interindividual variation in exposure existed,[18] which could, in turn, lead to

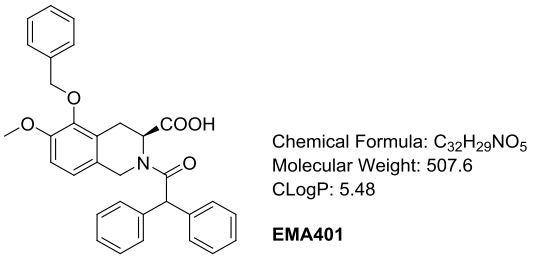

Figure 1. Structure of **EMA401**.

Received: April 8, 2021
Accepted: May 10, 2021
Published: May 28, 2021

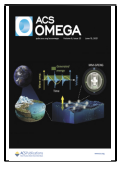

ACS Publications

© 2021 The Authors. Published by American Chemical Society

https://doi.org/10.1021/acsomega.1c01866
ACS Omega 2021, 6, 15412−15420

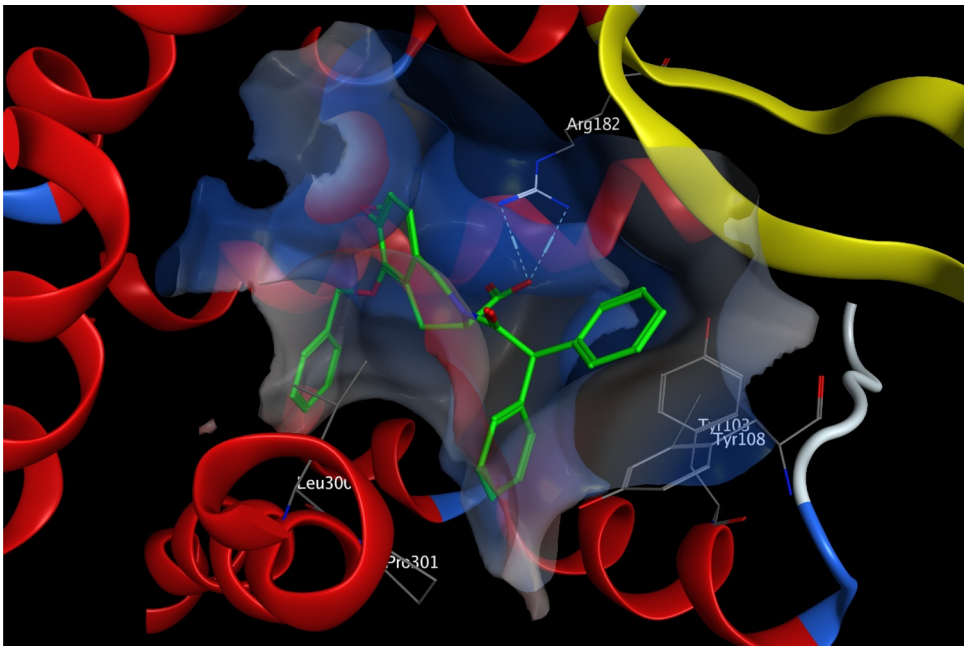

Figure 2. Docking model of **EMA401** binding to AT_2R (PDB, 5UNF). AT_2R in ribbons with the interaction surface colored by electrostatics, some key residues shown in sticks with carbon in gray, and **EMA401** in sticks with carbon in green.

variation in therapeutic effects in patients. Our aim was to develop a potent AT_2R antagonist with an improved pharmacokinetic profile. Herein, we report the design, synthesis, and biological activities of a novel series of benzoxazoles as potent and selective AT_2R antagonists and the *in vitro* and *in vivo* evaluation of the derived analogues, including a rat chronic constriction injury (CCI) model.

Our medicinal chemistry efforts started from **EMA401**. **EMA401** is an oily compound with *C* Log *P* as high as 5.48, and the diphenylacetyl moiety presumably contributes a lot to the high lipophilicity of the molecule. Docking of **EMA401** to the crystal structure of AT_2R[22] reveals that while one of the two geminal phenyl groups is well fitted into a hydrophobic pocket formed by Tyr103, Tyr108, Leu300, and Pro301, the other one is much more solvent-exposed (Figure 2), which indicates that the diphenylacetyl moiety as a whole probably is not ideal for protein−ligand interaction, and may be amenable to substitution.

RESULTS AND DISCUSSION

Our initial plan was to replace the diphenylacetyl of **EMA401** with benzoheteroaromatic groups to maintain the possible hydrophobic interaction with AT_2R and at the same time to reduce the lipophilicity of the small molecule (Table 1). Compounds **1**−**34** were synthesized as outlined in Schemes 1 and 2. Compounds **1**−**11** were readily synthesized as racemates. The isoquinoline **35**[23] was assembled to give **1a**−**11a** via S_NAr reaction with heteroaryl halides or oxidative amination of benzoxazoles.[24] Following saponification gave compounds **1**−**11**. Enantiopure intermediate **41** was synthesized according to the procedures similar to others.[25] Horner−Wadsworth−Emmons reaction of aldehyde **36** with phosphonate **37** followed by asymmetric catalytic hydrogenation[26] produced **39** with high *S*-enantioselectivity (98.7% ee). Deprotection of *tert*-butyloxycarbonyl gave **40**, which was further cyclized to **41** via a Pictet−Spengler reaction. S_NAr displacement of heteroaryl halides with **41** followed by saponification afforded the desired compounds **12**−**19**. The intermediates **14a** and **15a** could be further debenzylated to give phenols **42** and **43**, respectively. The following alkylation with various arylmethyl halides under basic conditions or with arylmethyl alcohols under Mitsunobu reaction conditions yielded compounds **20a**−**34a**, and subsequent saponification of the resulting esters produced the final compounds **20**−**34**. It was worth noting that compound **15** was prepared from **36** and **37** through six steps with high yield (57% overall yield) and high enantiomeric excess (98.5% ee). Details on the synthesis of all compounds are described in the Supporting Information.

Here, we adopted a homogeneous time-resolved fluorescence (HTRF)-based competitive binding assay (see the Supporting Information for details) to measure the inhibitory activities of compounds of interest. **EMA401** had a half-maximum inhibitory concentration (IC_{50}) of 26 nM for human AT_2R (hAT_2R), which was in good agreement with that of 39 nM measured via a radiolabeled ligand-binding assay.[17] Replacement of the diphenylacetyl with quinazolin-4-yl led to complete activity loss (compound **1**). However, replacement with quinazolin-2-yl could restore the activity to the submicromolar level (compound **2**), which indicated that the orientation of this bicyclic aromatic ring was important. We then switched to [5,6]-bicyclic heteroaromatic rings. Benzonimidazol-2-yl (compound **3**) worsened the activity when compared to compound **2**. To our delight, benzothiazole-2-yl demonstrated decent activity, leading to compound **4** with an IC_{50} of around 200 nM. A more dramatic activity boost was seen for benzoxazole-2-yl; the resulting compound **5** showed comparable potency (IC_{50} = 64 nM) to **EMA401** (IC_{50} = 26 nM) and more than one-log reduction in lipophilicity. The encouraging result promoted further structure−activity relationship (SAR) studies on the benzoxazole ring. We first did a methyl-walk on the ring. It turned out that activity was very sensitive to the substitution position. The 6-Me compound **8** kept the potency with an IC_{50} value of 62 nM, while 4-Me (**6**),

https://doi.org/10.1021/acsomega.1c01866
ACS Omega 2021, 6, 15412−15420

Table 1. SAR of Diphenylacetyl Replacement for hAT$_2$R Antagonistic Activities

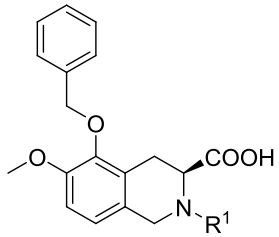

Compd.	R^1	M_w	CLogP	IC$_{50}$ (nM) [a]
EMA401		507.6	5.48	26 ± 12 (15)
1 [b]		441.5	4.07	>10000
2 [b]		441.5	4.07	885
3 [b]		429.5	4.37	2099
4 [b]		446.5	4.93	232
5 [b, c]		430.5	4.22	64
6 [b]		444.5	4.72	3234
7 [b]		444.5	4.72	516
8 [b, c]		444.5	4.72	62
9 [b]		444.5	4.72	2475
10 [b]		464.9	5.00	2148
11 [b]		464.9	5.00	1152
12		464.9	5.00	37
13		448.5	4.43	12 ± 1 (3)
14		448.5	4.43	90
15 [c]		455.5	3.80	25 ± 9 (4)
16		498.5	5.22	124
17		472.5	5.65	159
18		460.5	4.52	138
19		431.5	3.28	54

[a]IC$_{50}$ for human AT$_2$R with standard deviation and the number of runs in brackets if applicable. [b]Racemate. [c]IC$_{50}$ > 10 μM for human AT$_1$R.

5-Me (**7**), and 7-Me (**9**) resulted in 50-, 8-, and 39-fold activity loss, respectively, when compared to compound **5**. Similar trends were observed in the following cases of Cl- or F-substitution (compounds **10**−**12** for Cl and **13**−**14** for F). It was thus concluded that position-6 was the sweet spot for substitution, and the fluorine atom seemed to fit ideally to this position with compound **13** showing an even better activity than **EMA401** (12 vs 26 nM). Nevertheless, substituents with different sizes or electronegativities were explored at position-6 (compounds **15**−**18**). Size has been proven to matter more than the other factors; bulkier groups like CF$_3$ (**16**), ^{i}Pr (**17**), and OMe (**18**) were harmful, and more than 10-fold activity loss was observed when compared to corresponding fluorine compound **13**, while the smaller cyano group was well tolerated, leading to compound **15**, with an IC$_{50}$ of 25 nM and *C* Log *P* below 4. Furthermore, the hydrophilic pyridine analogue (**19**) provided similar potency to compound **5**. These results highlighted the delicate nature of the protein−ligand interaction at this region.

We next moved on to the exploration of the antagonistic ability of various arylmethyl derivatives of compounds **13** and **15** while maintaining a fluoro or a cyano substituent at the position-6 of the benzoxazole ring (Table 2). Substitution on the phenyl ring in general decreased antagonistic activities, with *p*-F (**24**, 17 nM), *p*-CF$_3$ (**26**, 11 nM), and *p*-MeO (**27**, 5.9 nM; **33**, 11 nM) as a few exceptions. It is worthy to point out that *p*-methoxyl substitution actually increased the activity to a single-digit nanomolar level. In addition, replacement of the phenyl ring with pyridine was tolerable, and a combination of pyridine and methoxyl gave (6-methoxypyridin-3-yl)methyl derivative **31** with a hAT$_2$R IC$_{50}$ of 6.6 nM.

With this new series of hAT$_2$R inhibitors in hand, we went on to measure their selectivities over the hAT$_1$R. Six compounds (**5**, **8**, **15**, **27**, **28**, and **33**) with different hAT$_2$R activities were picked for a competitive binding assay against hAT$_1$R. Gratifyingly, none of them showed any hAT$_1$R antagonistic activity at the highest tested concentration (10 μM).

Based on the potency and selectivity, compounds **13**, **15**, **27**, and **31** were selected for drug metabolism and pharmacokinetic (DMPK) evaluation in the rat (Table 3), given the fact that animal efficacy studies were planned to be carried out in the rat (*vide infra*). **EMA401** showed moderate clearance both *in vitro* and *in vivo*, moderate exposure, and low oral bioavailability in rats. In contrast, our compounds, which have smaller molecular weights and substantially lower lipophilicities, demonstrated superiority in all these DMPK parameters. Among the four compounds, compound **15** stood out. Compound **15** had the lowest *in vivo* clearance (1.7 mL/min/kg) and the longest half-life (4.2 h). Its exposure was excellent, and greater than 10- and 30-fold increases were realized in terms of C_{max} (6657 vs 470 ng/mL for **EMA401**) and AUC (44,100 vs 1470 (ng·h)/mL), respectively. Furthermore, its bioavailability was also significantly improved (47 vs 12% for **EMA401**).

Compound **15** was thus further evaluated by *in vitro* and *in vivo* experiments with **EMA401** as the comparator (Table 4). The metabolic stability of compound **15** was high in the human liver microsome and medium in human hepatocytes. However, **EMA401** had high clearance in both the liver microsome and hepatocytes of the human. A recent paper actually reported that **EMA401** was highly unstable in hepatocytes of many species, e.g., mouse, rat, dog, monkey, and human,[21] and glucuronidation was one of the predominant metabolism pathways. Both compounds had high plasma

https://doi.org/10.1021/acsomega.1c01866
ACS Omega 2021, 6, 15412−15420

Scheme 1. Synthetic Routes of Racemic Compounds 1−11[a]

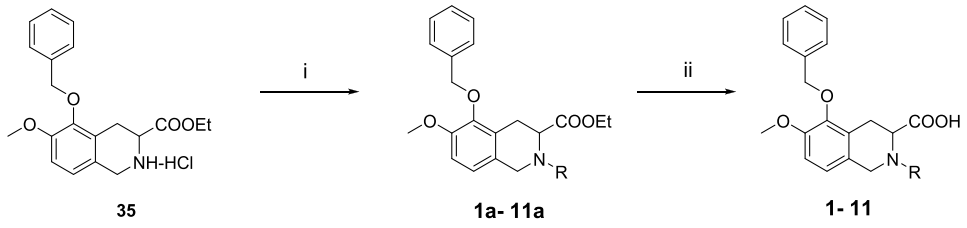

1a, 1, R = quinazolin-4-yl
2a, 2, R = quinazolin-2-yl
3a, 3, R = 1H-benzo[d]imidazol-2-yl
4a, 4, R = benzo[d]thiazol-2-yl
5a, 5, R = benzo[d]oxazol-2-yl
6a, 6, R = 4-methylbenzo[d]oxazol-2-yl
7a, 7, R = 5-methylbenzo[d]oxazol-2-yl
8a, 8, R = 6-methylbenzo[d]oxazol-2-yl
9a, 9, R = 7-methylbenzo[d]oxazol-2-yl
10a, 10, R = 4-chlorobenzo[d]oxazol-2-yl
11a, 11, R = 5-chlorobenzo[d]oxazol-2-yl

[a]Reagents and conditions: (i) (a) heteroaryl halide, DIPEA, NMP, 80 °C; or (b) heteroaryl halide, DIPEA, NMP, 80 °C, and then TFA, CH_2Cl_2, rt; or (c) heteroaryl halide, K_2CO_3, DMF, rt; or (d) benzoxazole, Ag_2CO_3, $PhCO_2H$, CH_3CN, 60 °C; (ii) (e) NaOH, H_2O, THF, MeOH, rt; or (f) LiOH, H_2O, THF, rt.

protein binding with a free fraction less than 0.1% in both the rat and human. Interestingly, although compound **15** had good cell permeability with no efflux as shown in the Caco-2 cell permeability test, **EMA401** had low permeability and a high efflux ratio of 7.6. Neither compound crossed the blood−brain barrier (BBB) following p.o. administration in rats, as demonstrated by their extremely low brain-to-plasma ratios. Nevertheless, the high efflux ratio of **EMA401** could partially contribute to its low bioavailability in different preclinical species. Compound **15** displayed no significant inhibition of six human CYP isozymes, including CYP1A2, CYP2C8, CYP2C9, CYP2C19, CYP2D6, and CYP3A4, while **EMA401** exhibited medium inhibition on CYP2C9 with an IC_{50} value of 7.4 μM. The drug−drug interaction assays indicated less liabilities in potential drug combination use for compound **15** than **EMA401**. In an *in vitro* cardiovascular safety evaluation, both compound **15** and **EMA401** indicated no hERG potassium channel activity at concentrations up to 10 μM, avoiding potential cardiovascular liability. The single-dose PK studies in dogs were also examined. Again, compound **15** showed a superior PK profile to **EMA401** with significant higher plasma exposure (>70-fold in AUC) and oral bioavailability (75 vs 39%).

As the AT_2R competitive binding assay is not enough evidence to claim agonistic or antagonistic effects of compounds, a neurite outgrowth functional assay was conducted in NG108-15 cells.[27] The functional assay showed that **EMA401** and compound **15** abolished neurite outgrowth induced by angiotensin II and confirmed that compound **15** had an antagonistic effect on AT_2R.

Given its most balanced overall profile, compound **15** was advanced to *in vivo* efficacy evaluation in the chronic constriction injury (CCI) rat model of neuropathic pain (Figure 3). The analgesic efficacy of compound **15** was assessed using von Frey filaments to measure paw withdrawal thresholds (PWT) in rats after p.o. administration. Pregabalin and **EMA401** were used as positive controls, and vehicle administration was used as the negative control. Mechanical allodynia was well developed in the ipsilateral hind paws of CCI rats at 13 days after CCI surgery, and the mechanical withdrawal threshold of the ipsilateral paws of CCI rats decreased to ∼6.5 g (PWT value) from a presurgery value of ∼13 g (see detailed experiments in the Supporting Information). A significantly increased paw withdrawal threshold responsive to tactile stimulation (von Frey) was observed in CCI rats orally dosed with compound **15**, pregabalin, and **EMA401**. A clear dose-dependent antiallodynia effect was exhibited at doses of 15, 30, and 60 mg/kg for compound **15**, and the duration of action at 30 and 60 mg/kg was about 2 h. Pregabalin showed a faster onset of action than compound **15** and **EMA401**, which probably was due to their different mechanisms of action and PK properties. Compound **15** at a dose of 30 mg/kg showed comparable efficacy to **EMA401** at the same dose, which was a bit unexpected given the fact that compound **15** should have much higher systemic exposure than **EMA401** at the same dosage. The difference in the tissue distribution profile or in free concentration at the action site between the two compounds may be a reason behind this discrepancy. In addition, although the two compounds showed comparable antagonistic activities toward the human AT_2R, their activities toward rat AT_2R were not measured due to the unavailability of a cell line expressing the rat AT_2R. Thus, between-species differences may also need to be investigated and should be taken as a critical step in compound screening cascades in the future.

Finally, a non-GLP 7-day acute rat toxicity study of compound **15** and **EMA401** was evaluated at multiple doses of 200, 400, and 800 mg/kg/day. Compound **15** and **EMA401** were well tolerated with no serious adverse events or significant laboratory abnormalities except for salivary discharge 1 h after dosage in high- and medium-dose groups for compound **15** and in high-, medium-, and low-dose groups for **EMA401**. The salivation phenomenon presented a dose-dependent effect, and the high-dose group of **EMA401** had the most severe salivation. There were no distinguishable gross anatomy differences in kidneys, hearts, or livers between treated groups (compound **15** and **EMA401**) and the vehicle group. AT_2R has a vital role in cardiovascular and renal systems. Although AT_2R knockout in mice increased the vasopressor response upon angiotensin II treatment and aggravated the impairment of renal function after renal injury,[28,29] AT_2R antagonists are unlikely to affect cardiovascular and renal functions under normal physiologic conditions. In adults, AT_2R is expressed at low levels in the normal cardiovascular system and kidneys.[3] It indicates that AT_2R antagonists might show no potential on-target toxicity in the

https://doi.org/10.1021/acsomega.1c01866
ACS Omega 2021, 6, 15412−15420

Scheme 2. Synthetic Routes of Compounds 16−34[a]

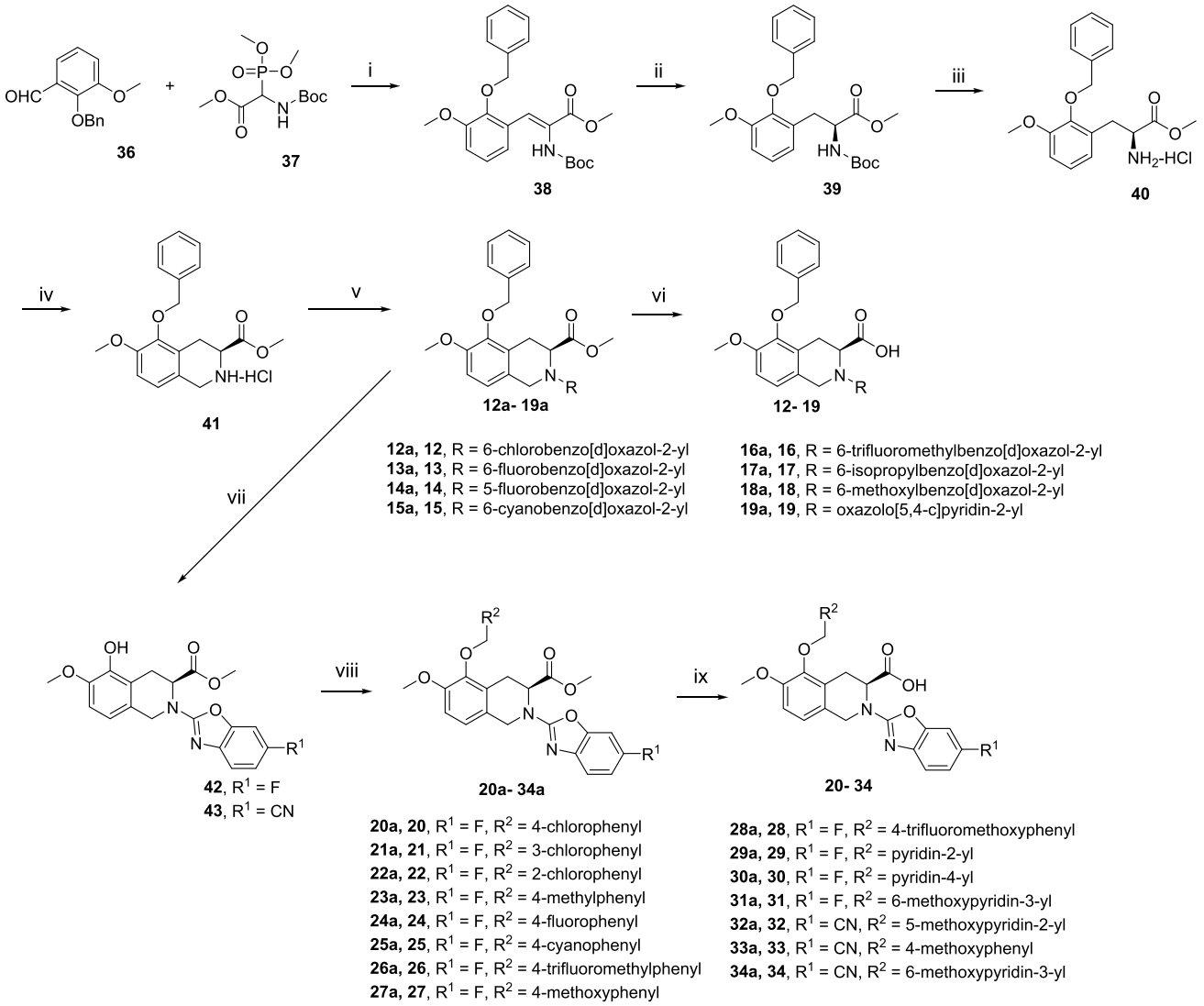

[a]Reagents and conditions: (i) 1,1,3,3-tetramethylguanidine, THF, rt, 88%; (ii) (*R*)-methyl BoPhoz, $[Rh(COD)_2]BF_4$, MeOH, H_2 rt; (iii) HCl, dioxane, rt, 96% for two steps; (iv) paraformaldehyde, HCl, dioxane, 70 °C, 82%; (v) (a) heteroaryl halide, Et_3N, THF, 60 °C; or (b) heteroaryl halide, K_2CO_3, DMF, rt; (vi) (c) LiOH, H_2O, THF, rt; or (d) $CaCl_2$, NaOH, H_2O, ^{i}PrOH, THF, rt; (vii) Pd/C, H_2, MeOH, rt; (viii) (e) $ArCH_2OH$, PPh_3, DIAD, THF, rt; or (f) $ArCH_2Cl$, K_2CO_3, NaI, DMF, rt; or (g) $ArCH_2Cl$, K_2CO_3, DMF, 70 °C; (ix) (h) LiOH, H_2O, THF, rt; or (j) $CaCl_2$, NaOH, H_2O, ^{i}PrOH, THF, rt.

heart and kidneys. However, two phase II clinical trials of **EMA401** have been terminated[30,31] very recently due to hepatotoxicity in monkeys after 39 weeks of chronic dosing,[32] which indicates that longer-term toxicity studies may be necessary for potential adverse effects.

CONCLUSIONS

In conclusion, we have discovered a series of potent AT_2R antagonists with benzoxazole side-chain based on **EMA401**. **EMA401** is metabolically highly unstable both *in vitro* and *in vivo*. Direct acylglucuronidation is the major elimination pathway, and the acyglucuronide metabolite was able to undergo acyl migration substantially under neutral conditions.[21] It was well documented that acylglucuronides could form covalent bonds with proteins and other bio-macromolecules, which may have a link with adverse drug reactions of some drugs.[33] However, it is too early to tell whether this metabolism pathway of **EMA401** had anything to do with the termination of two recent phase II clinical trials of **EMA401** due to safety concerns based on data from longer-term toxicity studies in monkeys. With the aim of improving the DMPK properties of **EMA401**, comprehensive rational optimization resulted in a novel series of compounds with high potencies, high selectivities over AT_1R, and more importantly with distinct improvement in drug-like properties, especially the liver microsome and hepatocyte stability. Compound **15** demonstrated an excellent PK profile in rodent/nonrodent species and analgesic efficacy in the CCI rat model. Further investigations including IND enabling studies and development of compound **15** are in progress and will be reported in due course.

EXPERIMENTAL SECTION

Chemistry. All materials, such as reagents, starting materials, and solvents, were purchased from commercial suppliers and were used without further purification. Reactions

https://doi.org/10.1021/acsomega.1c01866
ACS Omega 2021, 6, 15412−15420

Table 2. SAR of the Arylmethyl Ether Region

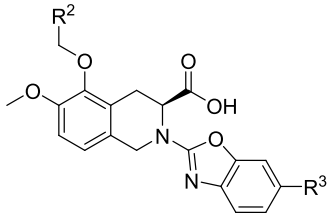

Compd.	R^2	R^3	M_w	CLogP	IC_{50}[a] (nM)
20		F	482.9	5.14	47
21		F	482.9	5.14	84
22		F	482.9	5.14	70
23		F	462.5	4.93	27
24		F	466.4	4.57	17
25		F	473.5	3.86	36
26		F	516.5	5.31	11
27[b]		F	478.5	4.35	5.9 ± 2. 6 (3)
28[b]		F	532.5	5.46	159
29		F	449.4	2.93	43
30		F	449.4	2.93	15
31		F	479.5	3.75	6.6
32		CN	486.5	2.73	33
33[b]		CN	485.5	3.72	11 ± 5 (5)
34		CN	486.5	3.13	46 ± 18 (3)

[a]IC_{50} for human AT_2R with standard deviation and the number of runs in brackets if applicable. [b]IC_{50} > 10 μM for human AT_1R.

were run under an argon atmosphere, unless noted otherwise. The reactions were monitored by thin-layer chromatography (TLC) and/or high-performance liquid chromatography-mass spectrometry (HPLC-MS). Analytical HPLC was performed on an Agilent 1200 (chromatographic column: Agilent Zorbax Eclipse Plus C18, 4.6 mm × 250 mm, 5 μm; T = 25 °C; λ = 245 nm; eluted with a 16 min gradient from 10 to 100% B, where A = H_2O/0.05% TFA and B = ACN; F = 1.0 mL/min). For NMR measurement, samples were dissolved in deuterated solvent (CD_3OD, $CDCl_3$, or DMSO-d_6), and spectra were acquired with a Bruker Avance-400 NMR spectrometer (^1H: 400 MHz; ^{13}C: 100 MHz) under standard observation conditions using tetramethylsilane (TMS) as an internal standard. The procedure for the synthesis of all compounds is given in the Supporting Information.

AT_2R and AT_1R Competitive Binding Assays. The AT_2R competitive binding assay was conducted in the Tag-lite angiotensin AT2 cells transiently expressing the angiotensin AT2 receptor labeled with terbium (Cisbio, catalog number: C1TT1AT2). Cryopreserved Tag-lite angiotensin AT2 cells (1 mL) were thawed in a 37 °C water bath, then transferred into a conical vial containing 5 mL of 1× Tag-lite buffer, centrifuged for 5 min at 300g, and resuspended in 2.7 mL of 1× Tag-lite buffer. 10 μL of labeled cells was dispensed into each well of a 384-well plate, and then 5 μL of reference compound (angiotensin II) or 5 μL of test compound solution (10-dose with a 5-fold serial dilution starting at 10 μM) and 5 μL of Tag-lite angiotensin receptor red agonist (Cisbio, catalog number: L0007RED, 12 nM in 1× Tag-lite buffer) were added to all assay wells. The assay plate was centrifuged for 1 min at 200g and incubated at 25 °C for 1 h. The data were read and collected on an EnVision (PerkinElmer, model: 2203-1060) by the HTRF-module. IC_{50} was calculated by Prism 5.0 software (GraphPad). AT_1R IC_{50} was determined by a similar assay with Tb-labeled Tag-lite AT_1 stable cells (Cisbio, catalog number: C1SU1AT1), and the reference compounds for the AT_1R binding assay were losartan and angiotensin II.

NG108-15 Neurite Outgrowth Assay. NG108-15 cells were purchased from the Cell Resource Center of the Institute of Basic Medical Sciences (IBMS) of the Chinese Academy of Medical Sciences and cultured in Dulbecco's modified Eagle medium (DMEM) with 10% fetal bovine serum and 2% HAT supplement (5 mM hypoxanthine, 20 μM aminopterin, 0.8 mM thymidine). For the neurite outgrowth assay, NG108-15 cells were plated in a 6-well plate at a density of 50,000 cells per well and incubated overnight. Cells were stimulated by 0.1 μM angiotensin II or co-treated with 0.1 μM angiotensin II and 1 μM compound (applied 30 min before angiotensin II) once a day for three consecutive days. The neurite outgrowth was observed and photographed using a microscope.

Chronic Constriction Injury (CCI) Model. Male Sprague−Dawley rats were subjected to peripheral neuropathy injury by constriction of the sciatic nerve.[34] Pain threshold base values were measured before and 13 days after surgery to check whether the model was successful. The rats were randomly separated into six groups (n = 8 per group). Pregabalin was used as the positive control, and the vehicle was used as the negative control. The rats were administered by

Table 3. *In Vitro* Metabolic Stability and PK Data of Compounds 13, 15, 22, and 31 in Rats[a]

		PK in rats					
compd.	CL_{int}[b]	C_{max}[c]	AUC_{0-24h}[c]	$T_{1/2}$[d]	CL[d]	Vd_{ss}[d]	F%[e]
EMA401	25.9 ± 1.0	470 ± 197	1470 ± 709	1.6 ± 0.3	14 ± 1	0.74 ± 0.1	12 ± 6%
13	12.5 ± 6.7	5280 ± 72	29,367 ± 4626	3.5 ± 0.3	2.1 ± 0.3	0.24 ± 0.05	36 ± 6%
15	8.13 ± 1.29	6657 ± 1745	44,100 ± 10,713	4.2 ± 1.2	1.7 ± 0.1	0.21 ± 0.06	47 ± 12%
27	10.4 ± 3.0	2370 ± 182	6930 ± 1720	2.4 ± 0.8	5.3 ± 1.0	0.37 ± 0.17	22 ± 5%
31	2.95 ± 0.18	5490 ± 1311	15,200 ± 2237	2.3 ± 0.4	5.0 ± 0.6	0.57 ± 0.06	45 ± 7%

[a]Units: CL_{int} (intrinsic clearance), mL/min/kg; C_{max}, ng/mL; AUC (area under the curve), (ng·h)/mL; $T_{1/2}$, h; CL (clearance), mL/min/kg; Vd_{ss} (steady-state apparent volume of distribution), L/kg. [b]Metabolic stability in the rat liver microsome. [c]p.o., 10 mg/kg. [d]i.v., 1 mg/kg. [e]F%, oral bioavailability.

https://doi.org/10.1021/acsomega.1c01866
ACS Omega 2021, 6, 15412−15420

Table 4. ADME, Early Safety, and Dog PK Data of Compound 15 and EMA401

compd.	15	EMA401
human liver microsome stability, CL_{int} (mL/min/kg)	1.50 ± 1.38	25.0 ± 1.1
human hepatocyte stability, CL_{int} (mL/min/kg)	26	66
plasma protein binding (PPB, rat/human)	>99.9%/>99.9%	>99.9%/>99.9%
brain-to-plasma ratio in the rat	0.012 ± 0.007	0.007 ± 0.001
Caco-2, P_{app}, A-B/B-A (10^{-6} cm/s)	11.3 ± 0.2/13.9 ± 0.3	3.3 ± 0.3/24.5 ± 1.5
CYP inhibition (1A2/2C8/2C9/2C19/2D6/3A4), IC_{50} (μM)	>50/>50/31/>50/>50/>50	>50/20/7.4/>50/>50/>50
hERG, IC_{50} (μM)	>10	>10
dog PK of sodium salt at 3 mg/kg, p.o.		
C_{max} (ng/mL)	19,500 ± 6366	2707 ± 1530
AUC_{0-t} ((ng·h)/mL)	132,483 ± 54,459	1727 ± 959
$T_{1/2}$ (h)	11 ± 3	2.3 ± 1.4
bioavailability (*F*%)	75 ± 31%	39 ± 22%

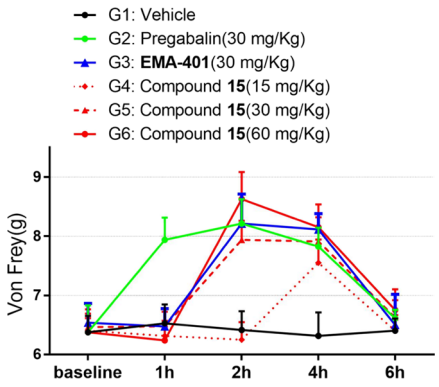

Figure 3. *In vivo* analgesic efficacy evaluation in the chronic constriction injury rat model after p.o. administration.

oral gavage at the indicated dose of test compounds as a suspension in 0.5% CMC-Na and 0.5% Tween 80 on the 14th day. Von Frey paw withdraw thresholds (PWT) were determined in the ipsilateral hind paws at the following times post-dosing: 1, 2, 4, and 6 h.

■ ASSOCIATED CONTENT

Supporting Information

The Supporting Information is available free of charge at https://pubs.acs.org/doi/10.1021/acsomega.1c01866.

Experimental details for synthetic procedures and analytical data; *in vitro* and *in vivo* assay information (PDF)

■ AUTHOR INFORMATION

Corresponding Authors

Yanghui Guo − *Shanghai Institute of Drug Discovery, Zhejiang Hisun Pharmaceutical Co., Ltd., Shanghai 201612, China*; orcid.org/0000-0003-0320-946X; Email: guoyh_sh@hisunpharm.com

Taishan Hu − *Shanghai Institute of Drug Discovery, Zhejiang Hisun Pharmaceutical Co., Ltd., Shanghai 201612, China*; Email: tshu@hisunpharm.com

Authors

Xiangui Huang − *Shanghai Institute of Drug Discovery, Zhejiang Hisun Pharmaceutical Co., Ltd., Shanghai 201612, China*

Weiwei Liao − *Shanghai Institute of Drug Discovery, Zhejiang Hisun Pharmaceutical Co., Ltd., Shanghai 201612, China*

Lichen Meng − *Shanghai Institute of Drug Discovery, Zhejiang Hisun Pharmaceutical Co., Ltd., Shanghai 201612, China*

Daiwang Xu − *Shanghai Institute of Drug Discovery, Zhejiang Hisun Pharmaceutical Co., Ltd., Shanghai 201612, China*

Cheng Ye − *Shanghai Institute of Drug Discovery, Zhejiang Hisun Pharmaceutical Co., Ltd., Shanghai 201612, China*

Lei Chen − *Shanghai Institute of Drug Discovery, Zhejiang Hisun Pharmaceutical Co., Ltd., Shanghai 201612, China; Zhejiang Hisun Pharmaceutical Co., Ltd., Taizhou, Zhejiang 318000, China*

Complete contact information is available at: https://pubs.acs.org/10.1021/acsomega.1c01866

Author Contributions

The manuscript was written through contributions of all authors. All authors have given approval to the final version of the manuscript.

Funding

These studies were funded by Zhejiang Hisun Pharmaceutical Co., Ltd.

Notes

The authors declare no competing financial interest.

■ ACKNOWLEDGMENTS

We thank the colleagues in the analytical group, biological group, and process group for their contributions on this work.

■ ABBREVIATIONS

AT_2R; angiotensin II type 2 receptor; AT_1R; angiotensin II type 1 receptor; PK; pharmacokinetic; CCI; chronic constriction injury; Tyr; tyrosine; Leu; leucine; Pro; proline; PDB; Protein Data Bank; HTRF; homogeneous time-resolved fluorescence; S_NAr; nucleophilic aromatic substitution; DIPEA; *N*,*N*-diisopropylethylamine; NMP; *N*-methyl pyrrolidone; TFA; trifluoroacetic acid; DMF; *N*,*N*-dimethylformamide; THF; tetrahydrofuran; DIAD; diisopropyl azodicarboxylate; SAR; structure−activity relationship; DMPK; drug metabolism and pharmacokinetic; CL_{int}; intrinsic clearance; CL; clearance; AUC; area under the curve; p.o.; per os; i.v.; intravenous injection; CYP; cytochrome P450 enzyme; hERG; human ether-a-go-go related gene; PPB; plasma protein binding; BBB; blood−brain barrier; Caco-2; human colorectal adenocarcinoma cell line; PWT; paw withdrawal thresholds; IND; investigational new drug; TLC; thin layer chromatography; HPLC; *high-performance liquid chromatography*; MS;

mass spectrometry; ACN; acetonitrile; NMR; nuclear magnetic resonance; DMSO; dimethyl sulfoxide; TMS; tetramethylsilane; DMEM; Dulbecco's Modified Eagle Medium; CMC-Na; sodium carboxymethyl cellulose

REFERENCES

(1) Karnik, S. S.; Unal, H.; Kemp, J. R.; Tirupula, K. C.; Eguchi, S.; Vanderheyden, P. M. L.; Thomas, W. G. International Union of Basic and Clinical Pharmacology XCIX. Angiotensin Receptors: Interpreters of Pathophysiological Angiotensinergic Stimuli. *Pharmacol. Rev.* **2015**, *67*, 754−819.

(2) de Gasparo, M.; Catt, K. J.; Inagami, T.; Wright, J. W.; Unger, T. International Union of Pharmacology XXIII. The Angiotensin II Receptors. *Pharmacol. Rev.* **2000**, *52*, 415−472.

(3) Juillerat-Jeanneret, L. The Other Angiotensin II Receptor: AT_2R as a Therapeutic Target. *J. Med. Chem.* **2020**, *63*, 1978−1995.

(4) Pulakat, L.; Sumners, C. Angiotensin Type 2 Receptors: Painful, or Not. *Front. Pharmacol.* **2020**, *11*, 571994.

(5) Hallberg, M.; Sumners, C.; Steckelings, U. M.; Hallberg, A. Small-molecule AT2 Receptor Agonists. *Med. Res. Rev.* **2018**, *38*, 602−624.

(6) Isaksson, R.; Lindman, J.; Wannberg, J.; Sallander, J.; Backlund, M.; Baraldi, D.; Widdop, R.; Hallberg, M.; Åqvist, J.; Gutiérrez-de-Terán, H.; Gising, J.; Larhed, M. A Series of Analogues to the AT_2R Prototype Antagonist C38 Allow Fine Tuning of the Previously Reported Antagonist Binding Mode. *ChemistryOpen* **2019**, *8*, 114−125.

(7) Sallander, J.; Wallinder, C.; Hallberg, A.; Åqvist, J.; Gutiérrez-de-Terán, H. Structural Determinants of Subtype Selectivity and Functional Activity of Angiotensin II Receptors. *Bioorg. Med. Chem. Lett.* **2016**, *26*, 1355−1359.

(8) Anand, U.; Yiangou, Y.; Sinisi, M.; Fox, M.; MacQuillan, A.; Quick, T.; Korchev, Y. E.; Bountra, C.; McCarthy, T.; Anand, P. Mechanisms Underlying Clinical Efficacy of Angiotensin II Type 2 Receptor (AT_2R) Antagonist EMA401 in Neuropathic Pain: Clinical Tissue and in Vitro Studies. *Mol. Pain* **2015**, *11*, 38−49.

(9) Treede, R.-D.; Jensen, T. S.; Campbell, J. N.; Cruccu, G.; Dostrovsky, J. O.; Griffin, J. W.; Hansson, P.; Hughes, R.; Nurmikko, T.; Serra, J. Neuropathic Pain: Redefinition and a Grading System for Clinical and Research Purposes. *Neurology* **2008**, *70*, 1630−1635.

(10) van Hecke, O.; Austin, S. K.; Khan, R. A.; Smith, B. H.; Torrance, N. Neuropathic Pain in the General Population: a Systematic Review of Epidemiological Studies. *Pain* **2014**, *155*, 654−662.

(11) Colloca, L.; Ludman, T.; Bouhassira, D.; Baron, R.; Dickenson, A. H.; Yarnitsky, D.; Freeman, R.; Truini, A.; Attal, N.; Finnerup, N. B.; Eccleston, C.; Kalso, E.; Bennett, D. L.; Dworkin, R. H.; Raja, S. N. Neuropathic Pain. *Nat. Rev. Dis. Primers* **2017**, *3*, 17003.

(12) Meacham, K.; Shepherd, A.; Mohapatra, D. P.; Haroutounian, S. Neuropathic Pain: Central vs. Peripheral Mechanisms. *Curr. Pain Headache Rep.* **2017**, *21*, 28.

(13) Moore, R. A.; Wiffen, P. J.; Derry, S.; Toelle, T.; Rice, A. S. Gabapentin for Chronic Neuropathic Pain and Fibromyalgia in Adults. *Cochrane Database Syst. Rev.* **2014**, *4*, CD007938.

(14) Woolf, C. J.; Mannion, R. J. Neuropathic Pain: Aetiology, Symptoms, Mechanisms, and Management. *Lancet* **1999**, *353*, 1959−1964.

(15) Mathieson, S.; Maher, C. G.; McLachlan, A. J.; Latimer, J.; Koes, B. W.; Hancock, M. J.; Harris, I.; Day, R. O.; Billot, L.; Pik, J.; Jan, S.; Lin, C.-W. C. Trial of Pregabalin for Acute and Chronic Sciatica. *N. Engl. J. Med.* **2017**, *376*, 1111−1120.

(16) Hesselink, J. K.; Schatman, M. E. EMA401: an Old Antagonist of AT_2R for a New Indication in Neuropathic Pain. *J. Pain Res.* **2017**, *Volume 10*, 439−443.

(17) Smith, M. T.; Wyse, B. D.; Edward, S. R. Small Molecule Angiotensin II Type 2 Receptor (AT_2R) Antagonists as Novel Analgesics for Neuropathic Pain: Comparative Pharmacokinetic, Radioligand Binding, and Efficacy in Rats. *Pain Med.* **2013**, *14*, 692−705.

(18) Rice, A. S. C.; Dworkin, R. H.; McCarthy, T. D.; Anand, P.; Bountra, C.; McCloud, P. I.; Hill, J.; Cutter, G.; Kitson, G.; Desem, N.; Raff, M. EMA401, an Orally Administered Highly Selective Angiotensin II Type 2 Receptor Antagonist, as a Novel Treatment for Postherpetic Neuralgia: a Randomised, Double-Blind, Placebo-Controlled Phase 2 Clinical Trial. *Lancet* **2014**, *383*, 1637−1647.

(19) Smith, M. T.; Muralidharan, A. Targeting Angiotensin II Type 2 Receptor Pathways to Treat Neuropathic Pain and Inflammatory Pain. *Expert Opin. Ther. Targets* **2015**, *19*, 25−35.

(20) Smith, M. T.; Anand, P.; Rice, A. S. C. Selective Small Molecule Angiotensin II Type 2 Receptor Antagonist for Neuropathic Pain: Preclinical and Clinical Studies. *Pain* **2016**, *157*, S33−S41.

(21) Murgasova, R.; Carreras, E. T.; Suetterlin-Hachmann, M.; Torrao, L. R. S.; Kittelmann, M.; Alexandra, V.; Fredenhagen, A. Non-Clinical Characterization of the Disposition of EMA401, a Novel Small Molecule Angiotensin II Type 2 Receptor (AT_2R) Antagonist. *Biopharm. Drug Dispos.* **2020**, *41*, 166−183.

(22) Zhang, H.; Han, G. W.; Batyuk, A.; Ishchenko, A.; White, K. L.; Patel, N.; Sadybekov, A.; Zamlynny, B.; Rudd, M. T.; Hollenstein, K.; Tolstikova, A.; White, T. A.; Hunter, M. S.; Weierstall, U.; Liu, W.; Babaoglu, K.; Moore, E. L.; Katz, R. D.; Shipman, J. M.; Garcia-Calvo, M.; Sharma, S.; Sheth, P.; Soisson, S. M.; Stevens, R. C.; Katritch, V.; Cherezov, V. Structural Basis for Selectivity and Diversity in Angiotensin II Receptors. *Nature* **2017**, *544*, 327−332.

(23) Wakchaure, P. B.; Bremberg, U.; Wannberg, J.; Larhed, M. Synthesis of Enantiopure Angiotensin II Type 2 Receptor [AT_2R] Antagonist EMA401. *Tetrahedron* **2015**, *71*, 6881−6887.

(24) Cho, S. H.; Kim, J. Y.; Lee, S. Y.; Chang, S. Silver-Mediated Direct Amination of Benzoxazoles: Tuning the Amino Group Source from Formamides to Parent Amines. *Angew. Chem., Int. Ed.* **2009**, *48*, 9127−9130.

(25) McCarthy, T. D.; Naylor, A. Heterocyclic Compounds and Methods of Their Use. WO/2015/003223.

(26) Boaz, N. W.; Mackenzie, E. B.; Debenham, S. D.; Large, S. E.; Ponasik, J. A. Synthesis and Application of Phosphinoferrocenylaminophosphine Ligands for Asymmetric Catalysis. *J. Org. Chem.* **2005**, *70*, 1872−1880.

(27) Mahalingam, A. K.; Wan, Y.; Murugaiah, A. M.; Wallinder, C.; Wu, X.; Plouffe, B.; Botros, M.; Nyberg, F.; Hallberg, A.; Gallo-Payet, N.; Alterman, M. Selective Angiotensin II AT2 Receptor Agonists with Reduced CYP 450 Inhibition. *Bioorg. Med. Chem.* **2010**, *18*, 4570−4590.

(28) Hein, L.; Barsh, G. S.; Pratt, R. E.; Dzau, V. J.; Kobilka, B. K. Behavioural and Cardiovascular Effects of Disrupting the Angiotensin II Type-2 Receptor Gene in Mice. *Nature* **1995**, *377*, 744−747.

(29) Benndorf, R. A.; Krebs, C.; Hirsch-Hoffmann, B.; Schwedhelm, E.; Cieslar, G.; Schmidt-Haupt, R.; Steinmetz, O. M.; Meyer-Schwesinger, C.; Thaiss, F.; Haddad, M.; Fehr, S.; Heilmann, A.; Helmchen, U.; Hein, L.; Ehmke, H.; Stahl, R. A.; Böger, R. H.; Wenzel, U. O. Angiotensin II Type 2 Receptor Deficiency Aggravates Renal Injury and Reduces Survival in Chronic Kidney Disease in Mice. *Kidney Int.* **2009**, *75*, 1039−1049.

(30) U.S. National Library of Medicine. https://clinicaltrials.gov/ct2/show/NCT03094195.

(31) U.S. National Library of Medicine. https://clinicaltrials.gov/ct2/show/NCT03297294.

(32) Rice, A. S. C.; Dworkin, R. H.; Finnerup, N. B.; Attal, N.; Anand, P.; Freeman, R.; Piaia, A.; Callegari, F.; Doerr, C.; Mondal, S.; Narayanan, N.; Ecochard, L.; Flossbach, Y.; Pandhi, S. Efficacy and Safety of EMA401 in Peripheral Neuropathic Pain: Results of Two Randomised, Double-Blind, Phase 2 Studies in Patients with Postherpetic Neuralgia and Painful Diabetic Neuropathy. *Pain* **2021**, DOI: 10.1097/j.pain.0000000000002252.

(33) Sawamura, R.; Okudaira, N.; Watanabe, K.; Murai, T.; Kobayashi, Y.; Tachibana, M.; Ohnuki, T.; Masuda, K.; Honma, H.; Kurihara, A.; Okazaki, O. Predictability of Idiosyncratic Drug Toxicity Risk for Carboxylic Acid-Containing Drugs Based on the Chemical

https://doi.org/10.1021/acsomega.1c01866
ACS Omega 2021, 6, 15412−15420

Stability of the Acyl Glucuronide. *Drug Metab. Dispos.* **2010**, *38*, 1857−1864.
(34) Austin, P. J.; Wu, A.; Moalem-Taylor, G. Chronic Constriction of the Sciatic Nerve and Pain Hypersensitivity Testing in Rats. *J. Vis. Exp.* **2012**, *13*, e3393.

https://doi.org/10.1021/acsomega.1c01866
ACS Omega 2021, 6, 15412−15420